Title

Soluble Epoxide Hydrolase Derived Linoleic Acid Oxylipins, Small Vessel Disease Markers, and Neurodegeneration in Stroke

Journal

Journal of the American Heart Association, 12(1)

ISSN

2047-9980

Authors

Yu, Di
Liang, Nuanyi
Zebarth, Julia
et al.

Publication Date

2023-01-03

DOI

10.1161/jaha.122.026901

Peer reviewed

Journal of the American Heart Association

ORIGINAL RESEARCH

Soluble Epoxide Hydrolase Derived Linoleic Acid Oxylipins, Small Vessel Disease Markers, and Neurodegeneration in Stroke

Di Yu, MSc; Nuanyi Liang, PhD; Julia Zebarth, MSc; Qing Shen, PhD; Miracle Ozzoude, BSc; Maged Goubran, PhD; Jennifer S. Rabin, PhD; Joel Ramirez, PhD; Christopher J. M. Scott, MSc; Fuqiang Gao, MD; Robert Bartha, PhD; Sean Symons, MD; Seyyed Mohammad Hassan Haddad, PhD; Courtney Berezuk, PhD; Brian Tan, MSc; Donna Kwan, PhD; Robert A. Hegele, MD; Allison A. Dilliott, PhD; Nuwan D. Nanayakkara, PhD; Malcolm A. Binns, PhD; Derek Beaton, PhD; Stephen R. Arnott, PhD; Jane M. Lawrence-Dewar, PhD; Ayman Hassan, MD; Dar Dowlatshahi, MD, PhD; Jennifer Mandzia, MD, PhD; Demetrios Sahlas, MD; Leanne Casaubon, MD, MSc; Gustavo Saposnik, MD, MSc; Yurika Otoki, PhD; Krista L. Lanctôt, PhD; Mario Masellis, MD, PhD; Sandra E. Black, MD; Richard H. Swartz, MD, PhD; Ameer Y. Taha, PhD; Walter Swardfager, PhD; The ONDRI Investigators*

BACKGROUND: Cerebral small vessel disease is associated with higher ratios of soluble-epoxide hydrolase derived linoleic acid diols (12,13-dihydroxyoctadecenoic acid [DiHOME] and 9,10-DiHOME) to their parent epoxides (12(13)-epoxyoctadecenoic acid [EpOME] and 9(10)-EpOME); however, the relationship has not yet been examined in stroke.

METHODS AND RESULTS: Participants with mild to moderate small vessel stroke or large vessel stroke were selected based on clinical and imaging criteria. Metabolites were quantified by ultra-high-performance liquid chromatography–mass spectrometry. Volumes of stroke, lacunes, white matter hyperintensities, magnetic resonance imaging visible perivascular spaces, and free water diffusion were quantified from structural and diffusion magnetic resonance imaging (3 Tesla). Adjusted linear regression models were used for analysis. Compared with participants with large vessel stroke (n=30), participants with small vessel stroke (n=50) had a higher 12,13-DiHOME/12(13)-EpOME ratio (β=0.251, *P*=0.023). The 12,13-DiHOME/12(13)-EpOME ratio was associated with more lacunes (β=0.266, *P*=0.028) but not with large vessel stroke volumes. Ratios of 12,13-DiHOME/12(13)-EpOME and 9,10-DiHOME/9(10)-EpOME were associated with greater volumes of white matter hyperintensities (β=0.364, *P*<0.001; β=0.362, *P*<0.001) and white matter MRI-visible perivascular spaces (β=0.302, *P*=0.011; β=0.314, *P*=0.006). In small vessel stroke, the 12,13-DiHOME/12(13)-EpOME ratio was associated with higher white matter free water diffusion (β=0.439, *P*=0.016), which was specific to the temporal lobe in exploratory regional analyses. The 9,10-DiHOME/9(10)-EpOME ratio was associated with temporal lobe atrophy (β=−0.277, *P*=0.031).

CONCLUSIONS: Linoleic acid markers of cytochrome P450/soluble-epoxide hydrolase activity were associated with small versus large vessel stroke, with small vessel disease markers consistent with blood brain barrier and neurovascular-glial disruption, and temporal lobe atrophy. The findings may indicate a novel modifiable risk factor for small vessel disease and related neurodegeneration.

Key Words: lacunar stroke ■ oxylipin ■ small vessel disease ■ soluble epoxide hydrolase ■ white matter hyperintensity

Correspondence to: Walter Swardfager, University of Toronto, Department of Pharmacology & Toxicology, 1 King's College Circle, Toronto, M5S1A8 Canada. Email: w.swardfager@utoronto.ca

*A complete list of the ONDRI Investigators can be found in the Appendix at the end of the manuscript.

Supplemental Material is available at https://www.ahajournals.org/doi/suppl/10.1161/JAHA.122.026901

For Sources of Funding and Disclosures, see page 12.

JAHA is available at: www.ahajournals.org/journal/jaha

CLINICAL PERSPECTIVE

What Is New?

- In clinical stroke, linoleic acid markers of cytochrome P450/soluble-epoxide hydrolase activity in peripheral blood were higher in people with small vessel versus large vessel etiology.
- On imaging, these blood markers were associated with the extent of cerebral small vessel disease (volumes of white matter hyperintensities and perivascular spaces), markers of blood brain barrier disruption (white matter free water), and temporal lobe atrophy.

What Are the Clinical Implications?

- This lipid pathway represents a novel modifiable risk factor and may offer new potential to track and treat small vessel stroke and related neurodegeneration.

Nonstandard Abbreviations and Acronyms

CYP450	cytochrome P450
FW	free water diffusion
LVS	large vessel stroke
LA	linoleic acid
PVS	MRI-visible perivascular space
ONDRI	Ontario Neurodegenerative Initiative
SVS	small vessel stroke/lacunar stroke
sEH	soluble epoxide hydrolase
WMH	white matter hyperintensity

Ischemic stroke is heterogeneous, involving divergent contributing causes, risk factors, and underlying etiopathologies. Two common ischemic stroke subtypes involve small vessel occlusion and large-artery stenosis producing symptoms.[1] Small vessel stroke (SVS) is defined by subcortical infarcts (lacunes), with other markers of cerebral small vessel disease including white matter hyperintensities (WMH), microbleeds, and enlarged magnetic resonance imaging (MRI)-visible perivascular spaces (PVS)[2]; however, these features are also found commonly in people who present clinically with large vessel stroke (LVS). These pathological overlaps and heterogeneities complicate efforts to identify biomarkers in peripheral blood among clinical stroke cases that reveal specific biological pathways related to SVS.

Recently, patients with transient ischemic attack were found to have a metabolic signature in polyunsaturated fatty acid metabolism; specifically, higher metabolism of cytochrome P450 (CYP450) derived epoxides of linoleic acid (LA) into their diols was observed compared to controls.[3] This was shown by an elevated ratio of the 12,13-dihydroxyoctadecenoic acid (DiHOME) (diol) to the 12(13)-epoxyoctadecenoic acid (EpOME) (epoxide) in peripheral blood, which also correlated with WMH volume. Metabolism of fatty acid epoxides into their respective diols is catalyzed by soluble epoxide hydrolase (sEH), an enzyme found elevated in the small vessels of people with vascular dementia.[4] The association between LA diol/epoxide ratios and more WMH was confirmed subsequently in a nondemented hypertensive cohort.[5] In the transient ischemic attack study, patients with MRI evidence of large vessel disease were excluded, leaving the associations between WMH- and sEH-related LA diol/epoxide ratios still to be explored in clinical stroke populations and for it to be determined how diol/epoxide ratios would compare between stroke patients with SVS versus LVS etiologies.

The current study examines the association between the LA diol/epoxide ratios and cerebral small vessel disease in a clinical stroke population. We focused on the ratios of these LA diols/epoxides as biomarkers of soluble epoxide hydrolase activity because the LA epoxides and diols were previously found to be more abundant than those of other long-chain fatty acids, and they were detectable in 100% of participants.[3] We hypothesized that the LA diol/epoxide ratios would be higher in patients with SVS compared with patients with LVS and that the ratios would be associated with higher WMH volumes. We also hypothesized that the LA diol/epoxide ratios would correlate with more enlarged MRI-visible PVS and increased free water diffusion (FW) and gray matter atrophy (as the marker of neurodegeneration), which we explored to better characterize the relationship between LA oxylipins and small vessel disease (SVD).

METHODS

Study Participants

Requests to access the data set from qualified researchers trained in human subject confidentiality protocols may be submitted to Ontario Neurodegenerative Disease Research Initiative (ONDRI) at http://ondri.ca.

The study cohort is selected from the cerebrovascular disease cohort of a multicenter, longitudinal observational study – ONDRI. The cohort was selected based on the Trial of Org 10172 in Acute Stroke Treatment (TOAST) criteria,[1] in which the participants must either have stroke attributable to large-artery atherosclerosis (clinical and brain imaging findings of either significant [>50%] stenosis or occlusion of a major brain artery or branch cortical artery, presumably because of atherosclerosis), or strokes attributable to subcortical lacunar infarcts with lacunar syndromes

presented. TOAST subtypes were determined by neurologists based on their clinical syndromes and MRI features. Detailed inclusion and exclusion criteria for the ONDRI participants with cerebrovascular disease have previously been reported.[6] Briefly, participants aged between 55 and 85 years, with a Montreal Cognitive Assessment score ≥18, a history of mild to moderate stroke (≥3 months before study enrollment) but no history of baseline prestroke dementia, and sufficient proficiency in speaking and understanding English were recruited from various health centers across Ontario, Canada. Participants were excluded if they had severe cognitive impairment, aphasia, evidence of a nonvascular cause of symptoms, inability to write or severe functional disability, severe claustrophobia, or other contraindications to MRI scanning procedures or other assessments.[7] Participants with large cortical strokes (>1/3 middle cerebral artery) were excluded.[7] Ethics approval was obtained from all participating institutions and performed in accordance with the Declaration of Helsinki. All participants provided informed consent, and subsequently underwent clinical evaluation, MRI, and other assessments as part of the full ONDRI protocol.

Oxylipin Extraction and Quantification

The 4 LA oxylipins in the free (unesterified) pool were extracted through solid phase extraction then quantified through ultra-high-performance liquid chromatography–mass spectrometry/mass spectrometry, as described previously.[3,8] See Data S1 for detailed steps.

Neuroimaging

MRI was performed at 3.0 Tesla across 10 different MRI centers in Ontario using either Siemen scanners, General Electric scanners, or Philips scanners. T1-weighted, proton density/T2-weighted, fluid attenuated inversion recovery, diffusion tensor imaging (DTI) data were collected for quantifying the SVD markers and FW. MRI protocols were consistent with the Canadian Dementia Imaging Protocol[9] and were in compliance with the National Institute of Neurological Disorders and Stroke–Canadian Stroke Network Vascular Cognitive Impairment Harmonization Standards.[10]

All MRIs were initially evaluated by a neuroradiologist (S.S.) and processed using the previously published ONDRI neuroimaging pipeline.[11] Briefly, T1 images were used to initially quantify regional volumes of gray matter, white matter, ventricular, and sulcal cerebrospinal fluid. SVD markers (WMH, lacunes, PVS) were extracted from coregistered T1-weighted, and PD/T2-weighted images in compliance with the Standards for Reporting Vascular Changes on Neuroimaging.[2] WMHs were further divided in periventricular and deep, and lacunar infarcts were regionally delineated as subcortical or periventricular using a 3-dimensional connectivity approach. Cortico-subcortical stroke lesions were identified and verified by an expert research radiologist (F.G.) on T1-weighted and FLAIR images and manually traced under their supervision. Brain atrophy was assessed using the brain parenchymal fraction, defined as the ratio of brain parenchymal volume to total intracranial/regional volume, where smaller values indicate greater atrophy.[12] The final volumetric data were further subjected to a comprehensive quality control analysis pipeline using multivariate outlier detection algorithms for identification of anomalous observations.[13]

DTI data were corrected for field distortions and eddy current-induced distortions, as well as motion artifacts using FMRIB Software Library. Tensor fitting was conducted using a weighted-least squares approach, generating standard DTI scalar maps including fractional aniostropy (FA) and mean diffusivity (MD) maps (in the native T1-weighted image space). To perform FW mapping, the eddy current and motion-corrected diffusion MRI data were fitted to a 2-compartment diffusion model in each voxel, separating the FW from the non-FW tissue compartment.[14] An FW map represents the fractional volume (ranging from 0 to 1) of freely diffusing extracellular water with a fixed isotropic diffusivity of 3×10^{-3} mm^2/s (the diffusion coefficient of water at body temperature). The FW-corrected FA represents the FA signal following removal of the FW signal and is expected to be more specific to axonal changes than FA alone.[15] All diffusion maps were checked visually for quality assurance, and scans with excessive motion or artifacts were excluded. Subsequently, the mean FA, MD, FW, and FW-adjusted FA were extracted in the normal appearing white matter. The FreeSurfer pipeline[16,17] was used to extract regional diffusion metrics for exploratory analyses, through structural segmentation of the T1-weighted scan.

Statistical Analysis

Differences in demographics, comorbidities, and imaging markers between the group with LVS and SVS were compared using Student *t* or Chi-square tests (with the SVS group as group 1). Cohen *d* (continuous variables) or Cramer V (categorical variables) were presented as indicators of the size of the difference between the groups. A Cohen *d* of 0.2 is considered as a small effect size. Oxylipin species were compared between groups through independent sample *t*-tests. Diol/epoxide ratios were calculated and used as surrogate markers of sEH activity for hypothesis testing. Linear regression models were used to examine the association between the stroke subtypes and diol/epoxide ratios (dependent variable; FDR corrected for 2 comparisons at a rate of 10%), as well as the relationships between the diol/

epoxide ratios and SVD imaging markers, with age, sex, hyperlipidemia, fasting glucose, waist circumference, and use of polyunsaturated fatty acid supplement controlled. Covariates were chosen if they were known to affect the outcomes a priori, or if they differed significantly between the subgroups. In addition, regional markers were explored post hoc. All analyses were performed using SPSS (version 24).

RESULTS

Participant Characteristics

Based on the TOAST classification criteria, 80 patients with SVS (n=50) or LVS (n=30) were included in the study. The 2 groups were similar in demographic characteristics and concomitant medications (Table 1). Compared with the SVS group, participants with LVS had a higher rate of hyperlipidemia. On MRI, participants with SVS had smaller stroke lesion volumes but larger small vessel disease volumes, including WMH volume (deep and periventricular), and greater volumes of periventricular infarcts (Table 2).

Serum Oxylipin Concentrations

The concentration and detectability of 4 LA oxylipins derived from the CYPP450-sEH pathway are summarized in Table 3. All 4 species had a detectability of 100%, and 2 ratios (12,13-DiHOME/12(13)-EpOME, 9,10-DiHOME/9(10)-EpOME) were generated for hypothesis testing.

Associations Between Diol/Epoxide Ratios and Stroke Etiology

In a linear regression model controlling for potential confounding variables known to affect the outcome or that differed between the groups, SVS was associated with higher 12,13-DiHOME/12(13)-EpOME ratio (β=0.251, 95% CI [0.466–0.035], *P*=0.023; Figure 1A). Post hoc analyses controlling for additional covariates, including hypertension (β=0.250, 95% CI [0.466–0.034], *P*=0.024), systolic blood pressure (β=0.254, 95% CI [0.471–0.036], *P*=0.023), and *APOE 4* presence (β=0.250, 95% CI [0.467–0.033], *P*=0.025), did not alter the association between SVS and higher 12,13-DiHOME/12(13)-EpOME ratio. The ratio of 9,10-DiHOME/9(10)-EpOME was not significant in this sample (β=0.138, 95% CI [–0.089 to 0.365], *P*=0.230, Figure 1B).

In linear models, the ratio of 12,13-DiHOME/12(13)-EpOME was associated with greater lacunar infarct volumes in the deep (ie, superficial) white matter (β=0.266, 95% CI [0.029–0.503], *P*=0.028) but not in the periventricular white matter (β=0.144, 95% CI [–0.068 to 0.357], *P*=0.180). These associations were not significant for the ratio of 9,10-DiHOME/9(10)-EpOME (deep lacunes: β=0.163, 95% CI [–0.072 to 0.398], *P*=0.172; periventricular lacunes: β=0.162, 95% CI [–0.043 to 0.368], *P*=0.120).

The oxylipin ratios were not associated with large vessel stroke lesion volumes (12,13-DiHOME/12(13)-EpOME ratio β=0.371, 95% CI [–0.299 to 0.212], *P*=0.112; 9,10-DiHOME/9(10)-EpOME ratio: β=0.088, 95% CI [–0.373 to 0.120], *P*=0.721).

Associations Between LA Diol/Epoxide Ratios and Small Vessel Disease Markers

In adjusted linear regression models, the ratios of 12,13-DiHOME/12(13)-EpOME and 9,10-DiHOME/9(10)-EpOME were associated with WMH volumes (Figure 2A and 2C: 12,13: β=0.364, 95% CI [0.183–0.545], *P*<0.001; 9,10: β=0.362, 95% CI [0.188–0.538], *P*<0.001). In post hoc exploratory analyses, the association between both ratios and deep WMH (Figure S1A: 12,13-DiHOME/12(13)-EpOME ratio: β=0.367, 95% CI [0.151–0.583], *P*=0.001; Figure S1B: 9,10-DiHOME/9(10)-EpOME ratio: β=0.252, 95% CI [0.033–0.470], *P*=0.025) or periventricular WMH (Figure S1C: 12,13-DiHOME/12(13)-EpOME ratio: β=0.341, 95% CI [0.158–0.523], *P*<0.001; Figure S1D: 9,10-DiHOME/9(10)-EpOME ratio: β=0.354, 95% CI [0.179–0.529], *P*<0.001) stayed significant. When split into subgroups, the relationship between WMH and both ratios were consistent between SVS (Figure 2B and 2D: 12,13-DiHOME/12(13)-EpOME ratio: β=0.315, 95% CI [0.087–0.544], *P*=0.008; 9,10-DiHOME/9(10)-EpOME ratio: β=0.417, 95% CI [0.196–0.574], *P*<0.001) and LVS subgroups (Figure 2 Band 2D: 12,13-DiHOME/12(13)-EpOME ratio: β=0.314, 95% CI [–0.039 to 0.667], *P*=0.079; 9,10-DiHOME/9(10)-EpOME ratio: β=0.176, 95% CI [–0.216 to 0.578], *P*=0.355), although the associations did not reach significance in the LVS group.

Both LA ratios were associated with more PVS in the white matter (Figure 3A:12,13-DiHOME/12(13)-EpOME ratio: β=0.302, 95% CI [0.071–0.532], *P*=0.011; Figure 3C 9,10-DiHOME/9(10)-EpOME ratio: β=0.314, 95% CI [0.092–0.537], *P*=0.006) but not in the basal ganglia (12,13-DiHOME/12(13)-EpOME ratio: β=0.153, 95% CI [–0.070 to 0.376], *P*=0.176; 9,10-DiHOME/9(10)-EpOME ratio: β=0.106, *P*=0.570). Considering LVS and SVS subgroups, white matter PVS were associated with the 9,10-DiHOME/9(10)-EpOME ratio (Figure 3B: β=0.350, 95% CI [0.083–0.617], *P*=0.011) but not with the 12,13-DiHOME/12(13)-EpOME ratio (Figure 3D: β=0.255, 95% CI [–0.056 to 0.566], *P*=0.105), in the SVS group.

Associations Between LA Diol/Epoxide Ratios and White Matter FW

Diffusion MRI was performed on 75 of the participants (46 SVS and 29 LVS). The 12,13-DiHOME/12(13)-EpOME

Table 1. Participants Characteristics

	Large vessel stroke (n=30)	Small vessel stroke (n=50)	*t* or χ^2	*P* value	Cohen *d*/ Cramer V
Demographics					
Age, y	67.4±6.3	70.3±7.7	1.74	0.086	0.4
Sex (% women)	23%	34%	1.02	0.313	0.1
MoCA	25.8±2.7	25.4±3.1	−0.66	0.509	−0.2
Education, y	14.3±2.9	14.7±3.0	0.53	0.598	0.1
Race			0.05	0.824	0.03
White	80%	82%			
Asian	13%	8%			
Black	7%	10%			
Vascular comorbidities					
Hypertension	77%	80%	0.12	0.724	0.04
Diabetes	13%	32%	3.48	0.062	0.2
Hyperlipidemia	93%	74%	4.60	0.032*	0.2
Smoking			4.39	0.112	0.2
Yes	13%	8%			
Quit	57%	38%			
No	30%	54%			
Fasting glucose	5.7±0.8	6.1 ±1.5	1.45	0.152	0.3
HbA1c	5.8±0.7	6.1 ±0.9	1.52	0.134	0.4
Waist circumference	0.9±0.1	0.9 ±0.1	−1.22	0.226	−0.03
HDL	1.3±0.3	1.4 ±0.4	1.35	0.182	0.3
LDL	1.8±0.5	1.9 ±0.8	0.47	0.639	0.1
Triglycerides	1.3±0.8	1.2 ±0.7	−0.64	0.521	−0.1
Medications					
Antihypertensives	87%	86%	0.00	0.933	0.01
ACE inhibitors	47%	58%	0.97	0.325	0.1
ARBs	17%	30%	1.78	0.182	0.2
Antidiabetics	13%	30%	2.88	0.090	0.2
Metformin	13%	26%	1.80	0.180	0.2
DPP4 inhibitors	10%	14%	0.27	0.600	0.06
Antihyperlipidemic	90%	80%	1.38	0.240	0.1
Statins	90%	86%	0.27	0.600	0.06
Cholesterol	7%	8%	0.05	0.826	0.03
Uptake blockers					
Fish oil supplements	7%	10%	0.26	0.609	0.06

ACE indicates angiotensin-converting enzyme; DPP-4, dipeptidyl peptidase 4; HbA1c, glycated hemoglobin; HDL, high-density lipoprotein; LDL, low-density lipoprotein; MoCA, Montreal Cognitive Assessment.

*Reference group large vessel stroke.

ratio was associated with higher white matter FW (β=0.273, 95% CI [0.031–0.515], *P*=0.028). This result was found in the SVS group (Figure 4A: β=0.439, 95% CI [0.088–0.790], *P*=0.016) but not in the LVS group (Figure 4A: β=0.046, 95% CI [−0.391 to 0.484], *P*=0.829). A similar trend was found between 9,10-DiHOME/9(10)-EpOME ratio and white matter FW in the whole group (β=0.222, 95% CI [−0.013 to 0.457], *P*=0.063), and the association was significant in the SVS group (Figure 4B: β=0.371, 95% CI [0.067–0.675], *P*=0.018) but not the LVS group (Figure 4B: β=−0.107, 95% CI [−0.586 to 0.371], *P*=0.646).

In an exploratory regional analysis, the ratios were found to be associated with FW in temporal lobe regions (including the fusiform, the entorhinal cortex, the inferior temporal lobe, and the middle temporal lobe) but not the other regions (Table S1). Comparing the groups, associations were found in the SVS group but not in the LVS group (Table S2), and additional regions were also involved in the SVS group (middle frontal,

Table 2. Imaging Features

	Large vessel stroke (n=30)	Small vessel stroke (n=50)	*t*	*P* value	Cohen *d*
Cortical stroke volume, cc	10.57±16.07	0.94±4.21	−5.84	<0.001*	−0.9
WMH, cc			2.10	0.005*	
Deep WMH, cc	0.70±0.99	1.08±1.03	2.78	0.007*	0.5
Periventricular WMH, cc	5.88±8.30	12.17±15.49	2.75	0.007*	0.4
Lacunes, cc					
Deep lacune, cc	0.03±0.04	0.06±0.10	2.52	0.132	0.4
Periventricular lacune, cc	0.14±0.30	0.51±1.02	2.35	0.022*	0.4
Perivascular spaces, cc					
White matter perivascular spaces, cc	0.04±0.07	0.05±0.07	1.40	0.165	0.2
Basal ganglia perivascular spaces, cc	0.02±0.05	0.03±0.04	1.29	0.200	0.2
White matter free water (factional volume)	0.20±0.03	0.21±0.03	1.94	0.057	0.5
Brain parenchymal fraction (atrophy)	0.77±0.05	0.77±0.04	−0.24	0.808	−0.05

WMH indicates white matter hyperintensities.
*Significant at $P<0.05$.

superior parietal, lateral occipital, caudal anterior cingulate; Table S2).

Associations Between LA Diol/Epoxide Ratios and Atrophy

Consistent with the free water findings, in the SVS subgroup, the 9,10-DiHOME/9(10)-EpOME ratio was associated with smaller brain parenchymal fraction (greater atrophy) in the temporal lobe specifically (Figure 5B: β=−0.277, 95% CI [−0.527 to −0.027], P=0.031). A similar trend was also seen with the 12,13-DiHOME/12(13)-EpOME ratio (Figure 5A: β=−0.262, 95% CI [−0.545 to 0.021], P=0.069, which) did not reach statistical significance. Similar relationships were not seen with other regional or global brain parenchymal fraction (Table S3).

DISCUSSION

The present findings report an association between sEH related diol/epoxide ratios and cerebral small vessel injury in a clinical symptomatic stroke sample. People with stroke of small vessel etiology had a higher 12,13-DiHOME/12(13)-EpOME ratio than patients with large vessel stroke, and people with a higher 12,13-DiHOME/12(13)-EpOME ratio had higher volumes of lacunar infarcts in the deep white matter. These results add to the previous finding that patients with transient ischemic attack had higher LA oxylipin ratios compared with healthy elderly controls, regardless of a relatively small effect size, suggesting that sEH is involved in stroke clinically consistent with a lacunar etiology.[3] The results may have implications for the development of differential treatment and prevention strategies for different stroke subtypes.

The 12,13-DiHOME/12(13)-EpOME ratio here was associated with the volume of WMH of presumed vascular origin, independent of demographics (age and sex), presence of *APOE4* and vascular risk factors (hyperlipidemia, fasting glucose, waist circumference, hypertension). The standardized coefficient was substantial, which makes the relationship more likely to be clinically relevant. WMH are heterogeneous in origin and can involve venous collagenosis, arteriolosclerosis, demyelination, activation of glial cells, and damage to the ependymal lining of the ventricles.[18-20] A role of sEH in these processes is not known; however, sEH immunoreactivity is detected intensely in specialized ependymal cells of the choroid plexus and in the oligodendrocytes and surrounding neuropil of the white matter in humans.[21] Immunoreactivity is also detected, in the endothelial cells of small vessels, in the pial and meningeal arteries (endothelial cells) and arterioles (smooth muscle cells), and in neurons, oligodendrocytes, and some astrocytes throughout the brain,[4,21] suggesting the need for further investigation of a possible role in SVD.

Although the observed associations do not imply causation, several mechanisms relating CYP450-sEH pathway to small vessel pathology have been demonstrated. Increased sEH expression has been observed in rat models of cerebral ischemia, and sEH inhibition has been found to preserve white matter integrity after hypoperfusion.[22] sEH-derived diols disrupt tight junctions and kill pericytes in the small vessels of the retina,[23] and in a diabetes mouse model, a sEH inhibitor prevented blood brain barrier disruption.[24] For these reasons, we hypothesized that higher diol/epoxide ratios would be correlated with greater white matter free water diffusion, which is thought to indicate, at least in part, vasogenic edema secondary to blood

Table 3. Concentrations of the 4 Quantified P450/sEH-Derived Oxylipins (nM)

Oxylipins	Abbreviation	Small vessel, stroke; median (IQR, nm) or %	Large vessel stroke; median (IQR, nm) or %	*t*	*P* value	Cohen *d*
9(10)-Epoxyoctadecamonoenoic acid	9(10)-EpOME	2.78 (2.25)	2.82 (1.85)	0.333	0.740	−0.002
9,10-Dihydroxyoctadecamonoenoic acid	9,10-DiHOME	1.34 (1.29)	1.00 (1.88)	1.853	0.068	0.2
9,10-DiHOME/9(10)-EpOME ratio		0.54 (0.79)	0.47 (0.59)	1.546	0.126	0.3
12(13)-Epoxyoctadecamonoenoic acid	12(13)-EpOME	5.63 (3.53)	6.22 (5.68)	−1.154	0.252	−0.4
12,13-Dihydroxyoctadecamonoenoic acid	12,13-DiHOME	4.80 (4.40)	4.45 (5.66)	1.388	0.169	0.1
12,13-DiHOME/12(13)-EpOME ratio		0.90 (0.85)	0.62 (0.84)	2.276	0.013*	0.4

DiHOME indicates dihydroxyoctadecenoic acid; EpOME, epoxyoctadecenoic acid; IQR, interquartile range; and sEH, soluble epoxide hydrolase.
*Significance was determined based on $P<0.025$, as 2 ratios were generated for hypothesis testing.

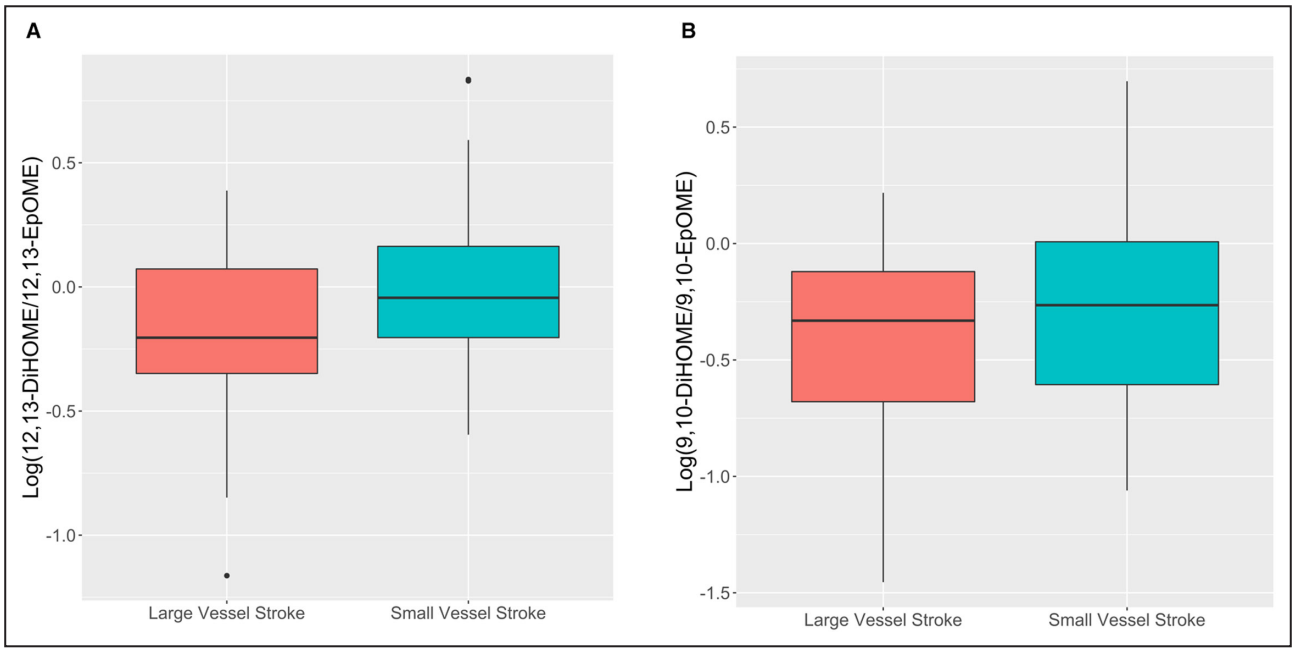

Figure 1. Differences in the ratios of 12,13-DiHOME/12(13)-EpOME (A, adjusted $F_{1,79}=5.39$, $P=0.023$) and 9,10-DiHOME/9(10)-EpOME (B, adjusted $F_{1,79}=1.46$, $P=0.230$) between patients with large vessel stroke (red) and small vessel stroke (blue). DiHOME indicates dihydroxyoctadecenoic acid; and EpOME, epoxyoctadecenoic acid.

brain barrier disruption in SVD.[25,26] This novel association was found, specifically in people with SVS. In a postmortem study of people with vascular cognitive impairment, the endothelial cells of the small vessels showed enhanced sEH immunoreactivity, specifically in small vessels proximal to cortical microinfarcts,[4] suggesting a specific role in small vessel disease. The lack of association between oxylipins and FW in LVS could be attributed to less involvement of small vessel injury in people who have predominantly large vessel occlusion. Nonetheless, people with LVS had some, albeit smaller, volumes of WMH and PVS, and effect sizes between oxylipin ratios and PVS and WMH were consistent between SVS and LVS groups. It should be considered that SVD markers are predictive of recurrent LVS,[27] suggesting that biological processes related to SVD may be clinically relevant, if indirectly, across stroke subtypes; the 12,13-DiHOME/12(13)-EpOME ratio showed a small-medium effect size for stroke lesion volume, but it was not significant, possibly because of small sample size, which should be investigated in larger studies.

Enlarged perivascular spaces are thought to indicate SVD, and more specifically dysfunction of glymphatic or perivascular interstitial fluid drainage systems.[2] PVS enlargement has been seen in pericyte-deficient mice with blood brain barrier dysfunction and in patients with genetic predisposition to WMH.[28] This is the first report to suggest a relationship between CYP450/sEH oxylipins and MRI-visible PVS. The finding may be consistent with the previous observation of sEH staining in perivascular adventitial cells of the surface pial arterioles,[21] which

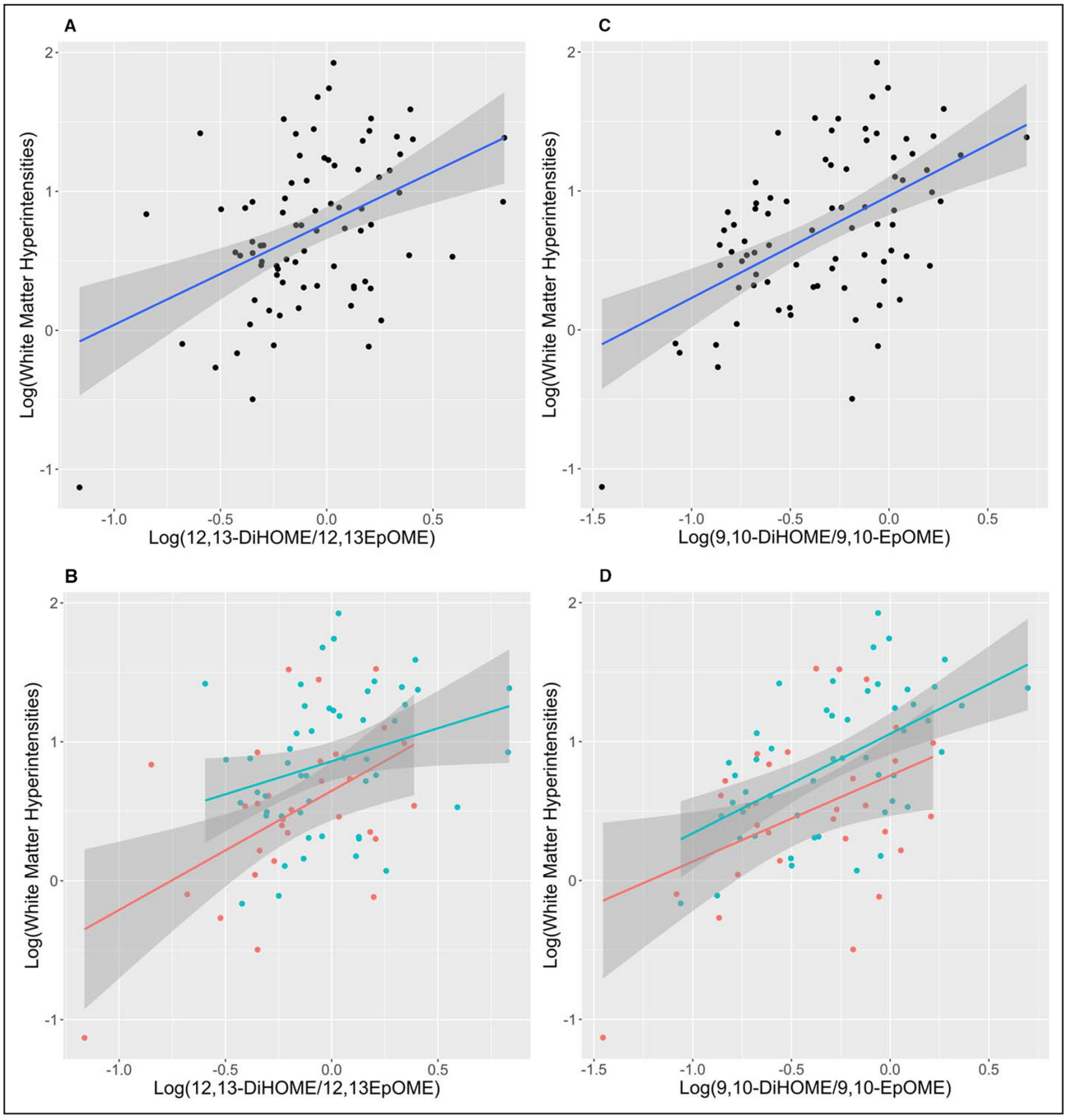

Figure 2. Associations between white matter hyperintensity volumes and the ratios of 12,13-DiHOME/12(13)-EpOME (A, β=0.364, 95% CI [0.183 to 0.545], *P*<0.001. B, β=0.314, 95% CI [−0.039 to 0.667], *P*=0.079) or the ratios of 9,10-DiHOME/9(10)-EpOME (C, β=0.362, 95% CI [0.188–0.538], *P*<0.001. D, β=0.176, 95% CI [−0.216 to 0.578], *P*=0.355) across the entire group (A and C) and within the small vessel stroke (blue) and large vessel stroke (red) subgroups (B and D). DiHOME indicates dihydroxyoctadecenoic acid; and EpOME, epoxyoctadecenoic acid.

may participate in glymphatic periarterial cerebrospinal fluid influx.[29] The present correlative evidence suggests involvement of sEH in neurovascular-glial unit dysfunction, and a need to determine whether manipulating this pathway might be beneficial.

Currently, therapeutic strategies under exploration to manipulate this pathway include sEH inhibitors to prolong beneficial activities of the epoxides and reduce the formation of cytotoxic diols,[30] or fatty acid epoxide mimetics.[31,32] In people with smoking and overweight, sEH inhibition was found to enhance peripheral vasodilatory function,[33] suggesting successful vascular target engagement in at-risk people and a need to investigate the effects of sEH inhibitors on cerebral circulation.

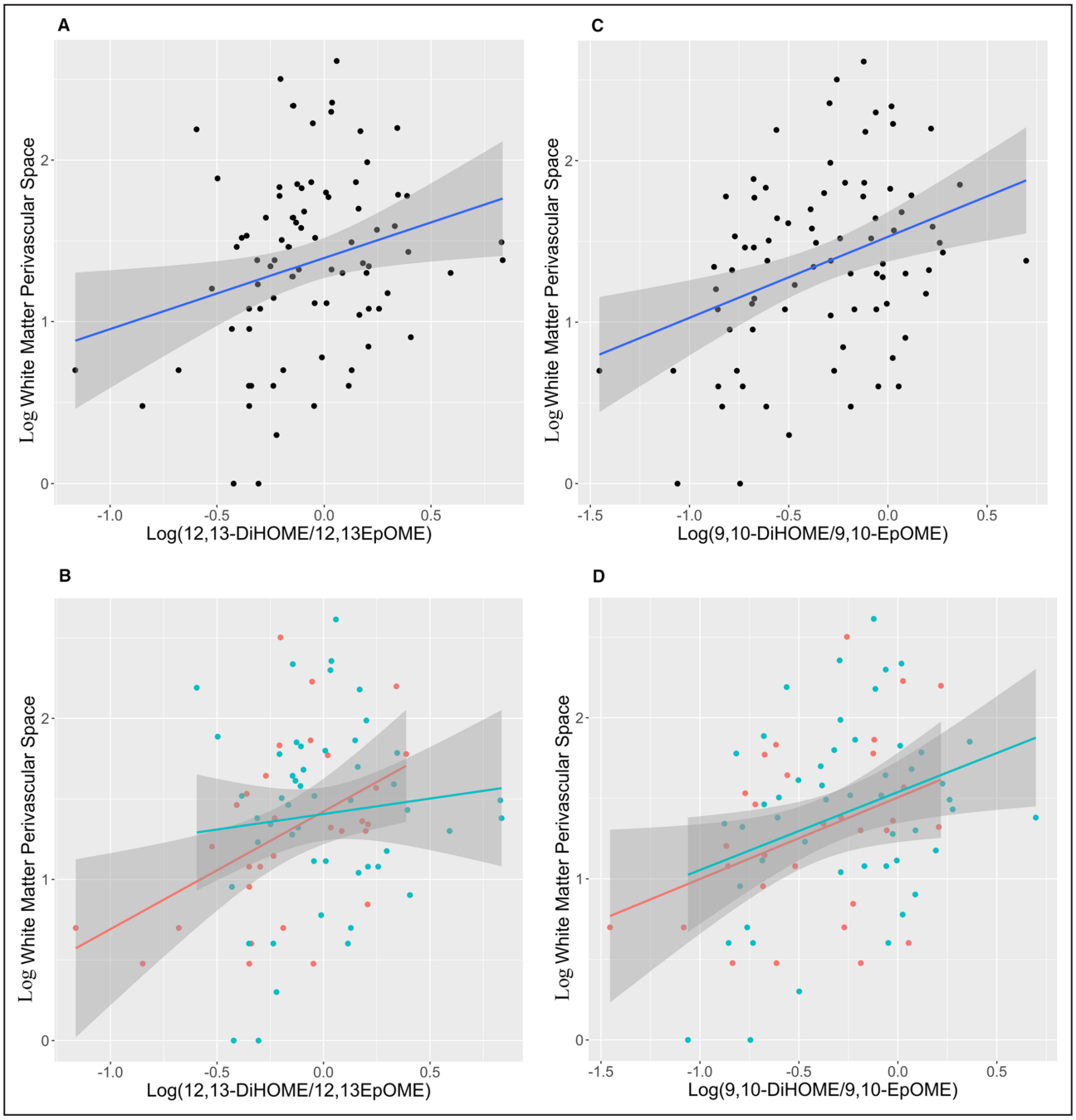

Figure 3. Association between white matter perivascular space and ratios of 12,13-DiHOME/12(13)-EpOME (A, β=0.302, 95% CI [0.071 to 0.532], *P*=0.011, B, β=0.350, 95% CI [0.083 to 0.617], *P*=0.011) or ratios of 9,10-DiHOME/9(10)-EpOME (C, β=0.314, 95% CI [0.092–0.537], *P*=0.006, D, β=0.255, 95% CI [−0.056 to 0.566], *P*=0.105) across the entire group (A and C) and within the small vessel stroke (blue) and large vessel stroke (red) subgroups (B and D). DiHOME indicates dihydroxyoctadecenoic acid; and EpOME, epoxyoctadecenoic acid.

Limitations and Future Directions

Concentrations of 12,13 species, but not of the 9,10 species, were similar to those observed previously in patients with transient ischemic attack and controls.[3] In contrast to the previous study, blood samples here were obtained fasting, which can affect these oxylipins,[34] and in mice, 9(10)-EpOME was more sensitive to diet compared with 12(13)-EpOME[35]; although correlations between the diol/epoxide ratios and SVD were generally robust, these implications for clinical biomarker development require further study. The linoleic acid diol/epoxide ratio might be interpreted as a

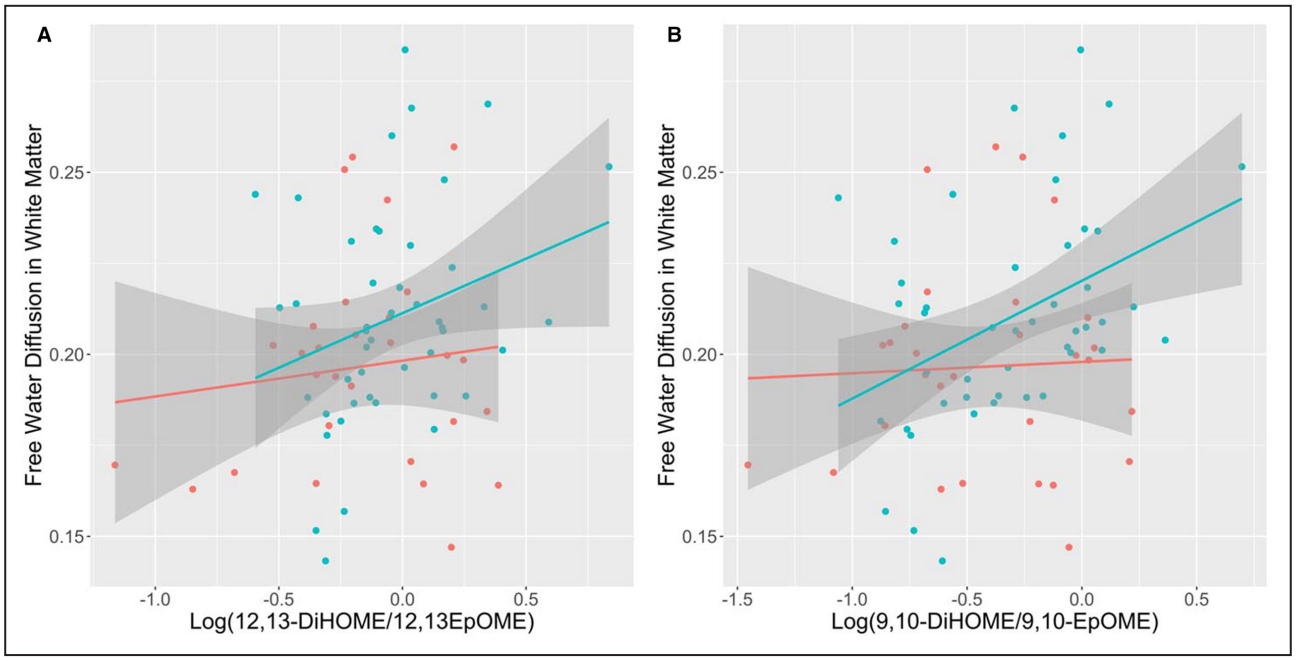

Figure 4. Associations between ratios of 12,13-DiHOME/12(13)-EpOME (A, small vessel stroke: β=0.439, 95% CI [0.088–0.790], *P*=0.016) or ratios of 9,10-DiHOME/9(10)-EpOME (B, small vessel stroke: β=0.371, 95% CI [0.067–0.675], *P*=0.018) and white matter free water fraction within the small vessel stroke (blue) and large vessel stroke (red) subgroups. DiHOME indicates dihydroxyoctadecenoic acid; and EpOME, epoxyoctadecenoic acid.

marker of soluble epoxide hydrolase activity. The present data do not indicate a causative adverse effect of linoleic acid diols or decreased linoleic acid epoxides specifically; the blood concentrations of these species overlap in those with small and large vessel stroke, as well as previously studied healthy controls.[3] Although

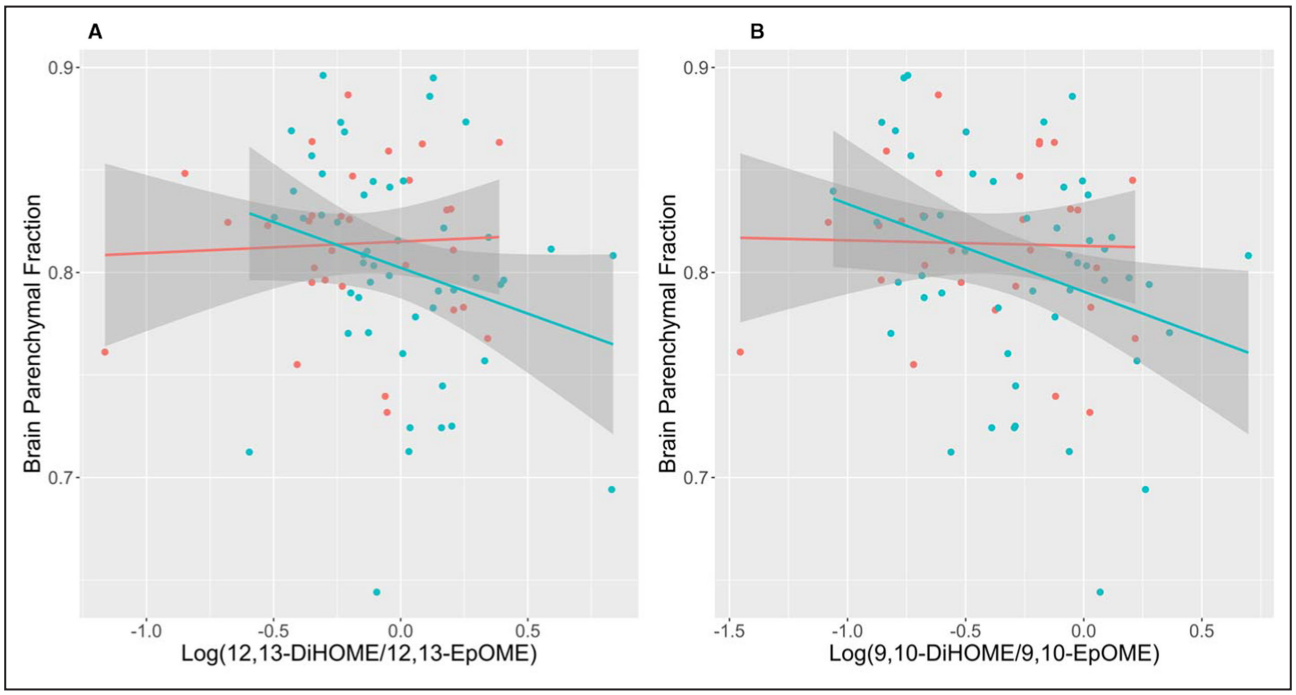

Figure 5. Associations between ratios of 12,13-DiHOME/12(13)-EpOME (A, small vessel stroke: β=−0.262, 95% CI [−0.545 to 0.021], *P*=0.069) or ratios of 9,10-DiHOME/9(10)-EpOME (B, small vessel stroke: β=−0.277, 95% CI [−0.527 to −0.027], *P*=0.031) and temporal lobe brain parenchymal fraction within the small vessel stroke (blue) and large vessel stroke (red) subgroups. DiHOME indicates dihydroxyoctadecenoic acid; and EpOME, epoxyoctadecenoic acid.

all main findings survived FDR correction, regional analyses post hoc were not corrected as they were exploratory, indicating a need for replication and further investigation. The diol/epoxide ratios showed particular correlations with free water diffusion in the temporal lobe, including the fusiform gyrus, entorhinal cortex, and throughout inferior and middle temporal regions. This potential regional differentiation was supported by another specific association identified between temporal lobe atrophy and the 9,10-DiHOME/9(10)-EpOME ratio, further suggesting that sEH markers were related to neurodegeneration in people with SVD,[25,36] suggesting the need for further studies to investigate associations with clinical features over time. The reason for these region-specific correlations is unclear; however, the temporal lobe is susceptible to small vessel damage and to pathological tau in preclinical[37,38] and early Alzheimer disease (AD).[39] In animal AD models, sEH gene deletion[40] or an sEH inhibitor[41] slowed AD progression; therefore, comparisons between oxylipins and AD biomarkers would be useful. Another regional difference was an association between PVS in the white matter but not in the basal ganglia, which might be attributable to the greater abundance of sEH in white matter or to anatomical differences between arterioles supplying blood to these regions. The arterioles supplying the basal ganglia tend to be larger, and PVS volumes there may reflect spaces around those larger vessels, which may be regulated differently than the pial arteries and deep penetrating arterioles that punctuate the neocortex.[42] Further studies would be needed to confirm these regional differences and to investigate mechanisms of vascular regulation and neurodegeneration and correlations with clinical progression. To establish better generalizability, further studies might also include a broader range of clinical stroke characteristics, including aphasia, which was excluded here.

CONCLUSIONS

The ratios of sEH derived LA diol to epoxide in the peripheral blood were different between patients with large versus small vessel stroke, and they were associated with the extent of cerebral small vessel disease markers (WMH and PVS) in patients with stroke. In small vessel stroke, the ratios were related to white matter free water diffusivity and to neurodegeneration having a potential proclivity for the temporal lobe. In the context of clinical stroke, these results suggest the involvement in the CYP450/sEH pathway in small vessel injury. The results suggest the need to explore sEH and related oxylipins as a potential target to treat small vessel disease.

APPENDIX

The ONDRI Investigators

Hurvitz Brain Sciences Program, Sunnybrook Research Institute, Toronto, Ontario, Canada: Natalie Rashkovan, Sandra E. Black, Agessandro Abrahao, Lorne Zinman, Alisia Bonnick, Richard H. Swartz, Mario Masellis, Joel Ramirez, Christopher Scott, Sean Symons, Courtney Berezuk, Melissa Holmes, Sabrina Adamo, Miracle Ozzoude.

Rotman Research Institute, Baycrest Health Sciences, Toronto, Ontario, Canada: Morris Freedman, Brian Tan, Mojdeh Zamyadi, Stephen Arnott, Derek Beaton, Malcolm Binns, Pradeep Raamana, Stephen Strother, Kelly Sunderland, Athena Theyers, Abiramy Uthirakumaran, Brian Levine, Angela Troyer.

Schulich School of Medicine & Dentistry, Western University, London, Ontario, Canada: Michael Strong, Peter Kleinstiver (retired), Michael Borrie, Elizabeth Finger, Christen Shoesmith, Frederico Faria, Manuel Montero-Odasso, Yanina Sarquis-Adamson, Alanna Black, Jennifer Mandzia, Allison Ann Dilliott, Rob Hegele, John Robinson, Sali Farhan.

Robarts Research Institute, Western University, London, Ontario, Canada: Rob Bartha, Hassan Haddad, Nuwan Nanayakkara, Guangyong (GY) Zou, Stephen Pasternak.

School of Communication Sciences and Disorders, Elborn College, Western University, London, Ontario, Canada: JB Orange, Angela Roberts.

London Health Sciences Centre, London, Ontario, Canada: Mandar Jog.

Queen's University, Kingston, Ontario, Canada: Dallas Seitz, Don Brien, Ying Chen, Brian Coe, Doug Munoz, Paula McLaughlin, Alicia Peltsch, Donna Kwan.

Dalla Lana School of Public Health, University of Toronto, Toronto, Ontario, Canada: Susan Bronskill, Wendy Lou.

Centre for Addiction and Mental Health, Toronto, Ontario, Canada: Sanjeev Kumar, Bruce Pollock, Tarek Rajji.

Department of Medicine, Division of Neurology, University of Toronto, Toronto, Ontario, Canada: David Tang-Wai.

Tanz Centre for Research in Neurodegenerative Disease, University of Toronto, Toronto, ON, Canada: Carmela Tartaglia.

Department of Emergency Medicine, University Health Network, Ontario, Canada: Brenda Varriano.

Faculty of Health Sciences, McMaster University, Hamilton, Ontario, Canada: Marvin Chum, John Turnbull.

Thunder Bay Regional Health Research Institute, Thunder Bay, Ontario, Canada: Jane Lawrence-Dewar, Ayman Hassan.

Centre for Community, Clinical and Applied Research Excellence, University of Waterloo, Waterloo,

Ontario, Canada: Julia Fraser, Bill McIlroy, Ben Cornish, Karen Van Ooteghem,

School of Optometry and Vision Science, University of Waterloo, Waterloo, Ontario, Canada:

Chris Hudson, Elena Leontieva.

Kensington Eye Institute, Toronto, Ontario, Canada: Wendy Hatch, Faryan Tayyari, Sherif Defrawy.

Department of Ophthalmology and Vision Sciences, University of Toronto, Toronto, ON, Canada. Edward Margolin.

Krembil Research Institute, Donald K Johnson Eye Institute, University Health Network, Toronto Ontario, Canada: Efrem Mandelcorn.

Department of Neurology, Johns Hopkins University School of Medicine, Baltimore, Maryland, United States of America: Barry Greenberg.

Toronto Western Hospital, Toronto, Ontario, Canada: Leanne Casaubon, Anthony Lang, Connie Marras.

Department of Medicine, Ottawa Hospital Research Institute, University of Ottawa, Ottawa, Ontario, Canada: Andrew Frank, Dar Dowlatshahi, David Grimes, Dennis Bulman, John Woulfe.

DisorDATA Analytics, Ottawa, Ontario, Canada: Mahdi Ghani.

Division of Neurology, Department of Medicine, Faculty of Health Sciences, McMaster University: Demetrios Sahlas.

Division of Neurology, St. Michael's Hospital, University of Toronto, Ontario, Canada: Gustavo Saposnik, Tom Steeves, David Munoz.

Keenan Research Centre for Biomedical Research, Li Ka Shing Knowledge Institute, St. Michael's Hospital, Toronto, Ontario, Canada: Corinne Fischer.

Tanz Centre for Research in Neurodegenerative Diseases, University of Toronto, Toronto, Ontario, Canada: Ekaterina Rogaeva.

Department of Ophthalmology & Visual Sciences, McGill University, Montreal, QC, Canada: Sujeevini Sujanthan.

Centre for Clinical Brain Sciences, University of Edinburgh, Edinburgh, United Kingdom: David Breen.

Neuroscience and Mental Health Institute, University of Alberta, Edmonton, Alberta, Canada. Roger A. Dixon.

ARTICLE INFORMATION

Received August 11, 2022; accepted November 14, 2022.

Affiliations

Dr. Sandra Black Center for Brain Resilience & Recovery, LC Campbell Cognitive Neurology, Hurvitz Brain Sciences Program, Sunnybrook Research Institute, Toronto, Canada (D.Y., J.Z., M.O., M.G., J.S.R., J.R., C.J.S., F.G., S.S., C.B., K.L.L., M.M., S.E.B., R.H.S., W.S.); Department of Pharmacology and Toxicology, University of Toronto, Toronto, Canada (D.Y., J.Z., K.L.L., W.S.); Department of Food Science and Technology, University of California, Davis, CA (N.L., Q.S., A.Y.T.); Harquail Centre for Neuromodulation, Sunnybrook Health Sciences Centre, Toronto, Canada (M.G., J.S.R.); Department of Medical Biophysics, University of Toronto, Toronto, Canada (M.G.); Division of Neurology, Department of Medicine, Sunnybrook Health Sciences Centre, Toronto, Canada (J.S.R., M.M., S.E.B., R.H.S.); Rehabilitation Sciences Institute, University of Toronto, Toronto, Canada (J.S.R.); Department of Medical Biophysics (R.B.); and Center for Functional and Metabolic Mapping, Robarts Research Institute (R.B., S.M.H.), Western University, London, Canada; Rotman Research Institute, Baycrest Health Sciences Centre, Toronto, Canada (B.T., M.A.B., D.B., S.R.A.); Centre for Neuroscience Studies, Queen's University, Kingston, Canada (D.K.); Robarts Research Institute, Western University, London, Canada (R.A.H., N.D.N.); Department of Neurology and Neurosurgery, McGill University, Montreal, Canada (A.A.D.); Dalla Lana School of Public Health, University of Toronto, Toronto, Canada (M.A.B.); Thunder Bay Regional Health Research Institute, Northern Ontario School of Medicine University, Thunder Bay, Canada (J.M.L., A.H.); Department of Medicine (Neurology), Ottawa Hospital Research Institute, University of Ottawa, Ottawa, Canada (D.D.); Department of Clinical Neurological Sciences, Schulich School of Medicine and Dentistry, Western University, London, Canada (J.M.); Division of Neurology, Department of Medicine, Faculty of Health Sciences, McMaster University, Hamilton, Canada (D.S.); Krembil Research Institute, University Health Network, Toronto, Canada (L.C.); Stroke Outcomes and Decision Neuroscience Research Unit, Division of Neurology, St. Michael's Hospital, University of Toronto, Toronto, Canada (G.S.); Division of Agricultural Chemistry, Graduate School of Agricultural Science, Tohoku University, Sendai, Japan (Y.O.); Department of Psychiatry, Faculty of Medicine, University of Toronto, Toronto, Canada (K.L.L.); Hurvitz Brain Sciences Program, Sunnybrook Research Institute, Toronto, Canada (K.L.L.); Department of Neurology, Faculty of Medicine, University of Toronto, Toronto, Canada (M.M., S.E.B., R.H.S.); and Toronto Rehabilitation Institute, University Health Network, Toronto, Canada (W.S.).

Acknowledgments

We thank the ONDRI participants for their time and participation in our study, and the ONDRI investigators (www.ONDRI.ca/people): the governing, executive, steering, publication, recruiting, assessment, and project management teams. We thank Drs Pasternak Ofer and Jordan Chad for providing the free water pipeline. RHS is supported by a Clinician–Scientist Phase II Award from Heart & Stroke. JRR and SEB acknowledge the Weston-Selfridges UK Brain Institute, the Fondation Leducq, the LC Campbell Foundation, the BrainLab.ca team, and the Sandra Black Centre for Brain Resilience and Recovery.

Sources of Funding

W. Swardfager gratefully acknowledges financial support from the Canadian Institute of Health Research (Team Grant); the Natural Sciences and Engineering Research Council of Canada (RGPIN-2017-06962); the Alzheimer's Association & Brain Canada (AARG501466); Weston Brain Institute & Alzheimer's Research UK, Alzheimer's Association, and Michael J. Fox Foundation (BAND3). The work was supported in part through funding from the Canada Research Chairs Program and the HSRLCE/CHFS/BI-Lilly Cardiometabolic Young Investigator's Award. A. Taha gratefully acknowledges the financial support from the Alzheimer's Association (2018-AARGD-591676). Y. Otoki is a recipient of a fellowship from the Japan Society for the Promotion of Science Core-to-Core Program, A (Advanced Research Networks entitled "Establishment of international agricultural immunology research-core for a quantum improvement in food safety"). This research was conducted with the support of the Ontario Brain Institute, an independent non-profit corporation, funded partially by the Ontario government. The opinions, results, and conclusions are those of the authors and no endorsement by the Ontario Brain Institute is intended or should be inferred. Matching funds were provided by participant hospital and research foundations, including the Baycrest Foundation, Bruyere Research Institute, Centre for Addiction and Mental Health Foundation, London Health Sciences Foundation, McMaster University Faculty of Health Sciences, Ottawa Brain and Mind Research Institute, Queen's University Faculty of Health Sciences, the Thunder Bay Regional Health Sciences Centre, the University of Ottawa Faculty of Medicine, and the Windsor/Essex County ALS Association. The Temerty Family Foundation provided the major infrastructure matching funds. The public web address for the ONDRI study may be given as www.ondri.ca

Disclosures

None.

Supplemental Material

Data S1
Tables S1–S3
Figure S1

REFERENCES

1. Adams HP Jr, Bendixen BH, Kappelle LJ, Biller J, Love BB, Gordon DL, Marsh EE. Classification of subtype of acute ischemic stroke. Definitions for use in a multicenter clinical trial. TOAST. Trial of org 10172 in acute stroke treatment. *Stroke.* 1993;24:35–41.
2. Wardlaw JM, Smith EE, Biessels GJ, Cordonnier C, Fazekas F, Frayne R, Lindley RI, O'Brien JT, Barkhof F, Benavente OR, et al. Neuroimaging standards for research into small vessel disease and its contribution to ageing and neurodegeneration. *Lancet Neurol.* 2013;12:822–838. doi: 10.1016/S1474-4422(13)70124-8
3. Yu D, Hennebelle M, Sahlas DJ, Ramirez J, Gao F, Masellis M, Cogo-Moreira H, Swartz RH, Herrmann N, Chan PC, et al. Soluble epoxide hydrolase-derived linoleic acid oxylipins in serum are associated with periventricular white matter hyperintensities and vascular cognitive impairment. *Transl Stroke Res.* 2019;10:522–533. doi: 10.1007/s12975-018-0672-5
4. Nelson JW, Young JM, Borkar RN, Woltjer RL, Quinn JF, Silbert LC, Grafe MR, Alkayed NJ. Role of soluble epoxide hydrolase in age-related vascular cognitive decline. *Prostaglandins Other Lipid Mediat.* 2014;113–115:30–37.
5. Shinto L, Lahna D, Murchison CF, Dodge H, Hagen K, David J, Kaye J, Quinn JF, Wall R, Silbert LC, et al. Oxidized products of Omega-6 and Omega-3 long chain fatty acids are associated with increased white matter hyperintensity and poorer executive function performance in a cohort of cognitively normal hypertensive older adults. *J Alzheimers Dis.* 2020;74:65–77. doi: 10.3233/JAD-191197
6. Farhan SMK, Bartha R, Black SE, Corbett D, Finger E, Freedman M, Greenberg B, Grimes DA, Hegele RA, Hudson C, et al. The Ontario neurodegenerative disease research initiative (ONDRI). *Can J Neurol Sci.* 2017;44:196–202. doi: 10.1017/cjn.2016.415
7. Sunderland KM, Beaton D, Arnott SR, Kleinstiver P, Kwan D, Lawrence-Dewar JM, Ramirez J, Tan B, Bartha R, Black SE, et al. Characteristics of the Ontario neurodegenerative disease research initiative cohort. *Alzheimer's & Dementia.* 2022;1–18.
8. Yang J, Schmelzer K, Georgi K, Hammock BD. Quantitative profiling method for oxylipin metabolome by liquid chromatography electrospray ionization tandem mass spectrometry. *Analyt Chem.* 2009;81:8085–8093. doi: 10.1021/ac901282n
9. Duchesne S, Chouinard I, Potvin O, Fonov VS, Khademi A, Bartha R, Bellec P, Collins DL, Descoteaux M, Hoge R, et al. The Canadian dementia imaging protocol: harmonizing national cohorts. *J Magn Reson Imaging.* 2019;49:456–465. doi: 10.1002/jmri.26197
10. Hachinski V, Iadecola C, Petersen RC, Breteler MM, Nyenhuis DL, Black SE, Powers WJ, DeCarli C, Merino JG, Kalaria RN, et al. National Institute of Neurological Disorders and Stroke-Canadian stroke network vascular cognitive impairment harmonization standards. *Stroke.* 2006;37:2220–2241. doi: 10.1161/01.STR.0000237236.88823.47
11. Ramirez J, Holmes MF, Scott CJM, Ozzoude M, Adamo S, Szilagyi GM, Goubran M, Gao F, Arnott SR, Lawrence-Dewar JM, et al. Ontario neurodegenerative disease research initiative (ONDRI): structural MRI methods and outcome measures. *Front Neurol.* 2020;11:847. doi: 10.3389/fneur.2020.00847
12. Vågberg M, Granåsen G, Svenningsson A. Brain parenchymal fraction in healthy adults—a systematic review of the literature. *PLOS ONE.* 2017;12:e0170018. doi: 10.1371/journal.pone.0170018
13. Sunderland KM, Beaton D, Fraser J, Kwan D, McLaughlin PM, Montero-Odasso M, Peltsch AJ, Pieruccini-Faria F, Sahlas DJ, Swartz RH, et al. The utility of multivariate outlier detection techniques for data quality evaluation in large studies: an application within the ONDRI project. *BMC Med Res Methodol.* 2019;19:102. doi: 10.1186/s12874-019-0737-5
14. Pasternak O, Sochen N, Gur Y, Intrator N, Assaf Y. Free water elimination and mapping from diffusion MRI. *Magn Reson Med.* 2009;62:717–730. doi: 10.1002/mrm.22055
15. Metzler-Baddeley C, O'Sullivan MJ, Bells S, Pasternak O, Jones DK. How and how not to correct for CSF-contamination in diffusion MRI. *Neuroimage.* 2012;59:1394–1403. doi: 10.1016/j.neuroimage.2011.08.043
16. Fischl B. FreeSurfer. *Neuroimage.* 2012;62:774–781. doi: 10.1016/j.neuroimage.2012.01.021
17. Ozzoude M, Ramirez J, Raamana PR, Holmes MF, Walker K, Scott CJM, Gao F, Goubran M, Kwan D, Tartaglia MC, et al. Cortical thickness estimation in individuals with cerebral small vessel disease, focal atrophy, and chronic stroke lesions. *Front Neurosci.* 2020;14:598868. doi: 10.3389/fnins.2020.598868
18. Sahlas DJ, Bilbao JM, Swartz RH, Black SE. Clasmatodendrosis correlating with periventricular hyperintensity in mixed dementia. *Ann Neurol.* 2002;52:378–381. doi: 10.1002/ana.10310
19. Black S, Gao F, Bilbao J. Understanding white matter disease: imaging-pathological correlations in vascular cognitive impairment. *Stroke.* 2009;40:S48–S52.
20. Keith J, Gao FQ, Noor R, Kiss A, Balasubramaniam G, Au K, Rogaeva E, Masellis M, Black SE. Collagenosis of the deep medullary veins: an underrecognized pathologic correlate of white matter hyperintensities and periventricular infarction? *J Neuropathol Exp Neurol.* 2017;76:299–312. doi: 10.1093/jnen/nlx009
21. Sura P, Sura R, Enayetallah AE, Grant DF. Distribution and expression of soluble epoxide hydrolase in human brain. *J Histochem Cytochem.* 2008;56:551–559. doi: 10.1369/jhc.2008.950659
22. Chen Y, Tian H, Yao E, Tian Y, Zhang H, Xu L, Yu Z, Fang Y, Wang W, Du P, et al. Soluble epoxide hydrolase inhibition promotes white matter integrity and long-term functional recovery after chronic hypoperfusion in mice. *Sci Rep.* 2017;7:1–14. doi: 10.1038/s41598-017-08227-z
23. Hu J, Dziumbla S, Lin J, Bibli S-I, Zukunft S, de Mos J, Awwad K, Frömel T, Jungmann A, Devraj K, et al. Inhibition of soluble epoxide hydrolase prevents diabetic retinopathy. *Nature.* 2017;552:248–252. doi: 10.1038/nature25013
24. Wu J, Zhao Y, Fan Z, Chen Q, Chen J, Sun Y, Jiang X, Xiao Q. Soluble epoxide hydrolase inhibitor protects against blood-brain barrier dysfunction in a mouse model of type 2 diabetes via the AMPK/HO-1 pathway. *Biochem Biophys Res Commun.* 2020;524:354–359. doi: 10.1016/j.bbrc.2020.01.085
25. Duering M, Finsterwalder S, Baykara E, Tuladhar AM, Gesierich B, Konieczny MJ, Malik R, Franzmeier N, Ewers M, Jouvent E, et al. Free water determines diffusion alterations and clinical status in cerebral small vessel disease. *Alzheimers Dement.* 2018;14:764–774. doi: 10.1016/j.jalz.2017.12.007
26. Ghosh M, Balbi M, Hellal F, Dichgans M, Lindauer U, Plesnila N. Pericytes are involved in the pathogenesis of cerebral autosomal dominant arteriopathy with subcortical infarcts and leukoencephalopathy. *Ann Neurol.* 2015;78:887–900. doi: 10.1002/ana.24512
27. Lau KK, Li L, Schulz U, Simoni M, Chan KH, Ho SL, Cheung RTF, Küker W, Mak HKF, Rothwell PM. Total small vessel disease score and risk of recurrent stroke: validation in 2 large cohorts. *Neurology.* 2017;88:2260–2267. doi: 10.1212/WNL.0000000000004042
28. Wardlaw JM, Benveniste H, Nedergaard M, Zlokovic B v, Mestre H, Lee H, Doubal FN, Brown R, Ramirez J, MacIntosh BJ, et al. Perivascular spaces in the brain: anatomy, physiology and pathology. *Nat Rev Neurol.* 2020;16:137–153. doi: 10.1038/s41582-020-0312-z
29. Bacyinski A, Xu M, Wang W, Hu J. The paravascular pathway for brain waste clearance: current understanding, significance and controversy. *Front Neuroanat.* 2017;11:101.
30. Goswami SK, Wan D, Yang J, Trindade Da Silva CA, Morisseau C, Kodani SD, Yang GY, Inceoglu B, Hammock BD. Anti-ulcer efficacy of soluble epoxide hydrolase inhibitor TPPU on diclofenac-induced intestinal ulcers. *J Pharmacol Exp Ther.* 2016;357:529–536. doi: 10.1124/jpet.116.232108
31. Falck JR, Koduru SR, Mohapatra S, Manne R, Atcha R, Manthati VL, Capdevila JH, Christian S, Imig JD, Campbell WB. 14,15-Epoxyeicosa-5,8,11-trienoic acid (14,15-EET) surrogates: carboxylate modifications. *J Med Chem.* 2014;57:6965–6972. doi: 10.1021/jm500262m
32. Falck JR, Koduru SR, Mohapatra S, Manne R, Atcha KR, Manthati VL, Capdevila JH, Christian S, Imig JD, Campbell WB. Correction to 14,15-Epoxyeicosa-5,8,11-trienoic acid (14,15-EET) surrogates: carboxylate modifications. *J Med Chem.* 2014;57:9218. doi: 10.1021/jm5016457
33. Yang L, Cheriyan J, Gutterman DD, Mayer RJ, Ament Z, Griffin JL, Lazaar AL, Newby DE, Tal-Singer R, Wilkinson IB. Mechanisms of vascular dysfunction in COPD and effects of a novel soluble epoxide hydrolase inhibitor in smokers. *Chest.* 2017;151:555–563. doi: 10.1016/j.chest.2016.10.058
34. Borkowski K, Taha AY, Pedersen TL, de Jager PL, Bennett DA, Arnold M, Kaddurah-Daouk R, Newman JW. Serum metabolomic biomarkers of perceptual speed in cognitively normal and mildly impaired subjects

with fasting state stratification. *Sci Rep.* 2021;11:18964. doi: 10.1038/s41598-021-98640-2
35. Taha AY, Hennebelle M, Yang J, Zamora D, Rapoport SI, Hammock BD, Ramsden CE. Regulation of rat plasma and cerebral cortex oxylipin concentrations with increasing levels of dietary linoleic acid. *Prostaglandins Leukot Essent Fatty Acids.* 2018;138:71–80. doi: 10.1016/j.plefa.2016.05.004
36. Swardfager W, Cogo-Moreira H, Masellis M, Ramirez J, Herrmann N, Edwards JD, Saleem M, Chan P, Yu D, Nestor SM, et al. The effect of white matter hyperintensities on verbal memory. *Neurology.* 2018;90:e673–e682. doi: 10.1212/WNL.0000000000004983
37. Kisler K, Nelson AR, Montagne A, Zlokovic BV. Cerebral blood flow regulation and neurovascular dysfunction in Alzheimer disease. *Nat Rev Neurosci.* 2017;18:419–434. doi: 10.1038/nrn.2017.48
38. Nation DA, Sweeney MD, Montagne A, Sagare AP, D'Orazio LM, Pachicano M, Sepehrband F, Nelson AR, Buennagel DP, Harrington MG, et al. Blood–brain barrier breakdown is an early biomarker of human cognitive dysfunction. *Nat Med.* 2019;25:270–276. doi: 10.1038/s41591-018-0297-y
39. Lin Z, Sur S, Liu P, Li Y, Jiang D, Hou X, Darrow J, Pillai JJ, Yasar S, Rosenberg P, et al. Blood–brain barrier breakdown in relationship to Alzheimer and vascular disease. *Ann Neurol.* 2021;90:227–238. doi: 10.1002/ana.26134
40. Lee H t, Lee KI, Chen CH, Lee TS. Genetic deletion of soluble epoxide hydrolase delays the progression of Alzheimer's disease. *J Neuroinflammation.* 2019;16:1–12.
41. Ghosh A, Comerota MM, Wan D, Chen F, Propson NE, Hwang SH, Hammock BD, Zheng H. An epoxide hydrolase inhibitor reduces neuroinflammation in a mouse model of Alzheimer's disease. *Sci Transl Med.* 2020;12:eabb1206.
42. Hurford R, Charidimou A, Fox Z, Cipolotti L, Jager R, Werring DJ. MRI-visible perivascular spaces: relationship to cognition and small vessel disease MRI markers in ischaemic stroke and TIA. *J Neurol Neurosurg Psychiatry.* 2014;85:522–525. doi: 10.1136/jnnp-2013-305815

SUPPLEMENTAL MATERIAL

Data S1.

Supplemental Methods

Oxylipin quantification

Briefly, 200µL ice-thawed serum were mixed with 10 µL surrogate standard (containing 2 µM each of d-11-11(12)EpETrE, d11-14,15-DiHETrE, d4-6-keto-PGF1a, d4-9HODE, d4-LTB4, d4-PGE2, d4-TXB2, d6-20-HETE and d8-5-HETE) and 610 µL extraction buffer (480 µL of 250 µM EDTA in water, 1 µL 10 % acetic acid in water and 120 µL of methanol containing 0.002% dibutylhydroxytoluene) before the extraction of the oxylipins. After vortexing and centrifuging the prepared samples for 15 min at 15,000 rpm, 0°C , the supernatant was loaded onto a tC18 Sep-Pak column (100 mg; Waters, Milford, MA, USA), which had been preconditioned with one column volume of methanol and two column volumes of 20% methanol. The column was then washed with 1.5 mL of 20% methanol followed by 1.5 mL of hexane. Oxylipins were then eluted using 2mL methanol. The eluted oxylipins were dried under nitrogen, reconstituted in 100 µL of methanol, and filtered.

The 4 LA oxylipins were analysed using an Agilent 1290 Infinity UHPLC system (Agilent Corporation, Palo Alto, CA, USA) connected to a 6460 Triple Quad tandem mass spectrometer (Agilent Corporation, Palo Alto, CA, USA) with an electrospray ionization source (Jet Stream technology). An Eclipse Plus C18, 2.1 × 150 mm, 1.8 µm column (Agilent Corporation, Palo Alto, CA, USA) with an Acquity 0.2 µm in-line filter (Walters, Milford, MA, USA) was used to separate the oxylipins. With the autosampler temperature maintained at 4 °C and the column at 45 °C, gradient elution was performed using pre-made solvent A (0.1% acetic acid (AcOH) in ultrapure water) and solvent B (acetonitrile/MeOH/AcOH (85/15/0.1%)) under an alternated flow rate:

- Solvent B was increased from 35 to 40% from 0 to 3 min, to 48% from 3 to 4 min, to 60% from 4 to 10 min, to 70% from 10 to 20 min, to 85% from 20 to 24 min, and to 99% from 24.5 to 24.6 min. Solvent B was then held at 99% for 4 min, decreased to 35% from 26 to 26.1 min, and held at 35% for 1.9 min.
- The flow rate started at 0.3 mL/min. It was decreased to 0.25 mL/min after 3 min, held at 0.25 mL/min for 21.6 min, increased to 0.35 mL/min at 24.6 min, and finally decreased to 0.3 mL/min at 27.3 min.

The instrument was operated in negative electrospray ionization mode throughout the analysis. After the LC-MS/MS, peaks were extracted and quantified using MassHunter Workstation -

Quantitative Analysis software (Agilent Technologies, Palo Alto, CA, USA). Extraction losses were corrected using the surrogate standards while adjusting for the response factor using the external standard calibration curve.

Table S1. Associations between LA diol/epoxide ratio and regional free water

Regional Free Water	Ratios	r (pearson coefficient)	p value
Entorhinal	12,13-ratio	0.225	0.053
	9,10-ratio	0.236	**0.041***
Fusiform	12,13-ratio	0.195	0.094
	9,10-ratio	0.29	**0.012***
Inferior temporal	12,13-ratio	0.243	**0.036***
	9,10-ratio	0.299	**0.009***
Middle temporal	12,13-ratio	0.16	0.169
	9,10-ratio	0.299	**0.009***
Hippocampus	12,13-ratio	-0.016	0.893
Hippocampus	9,10-ratio	0.054	0.643
Superior temporal	12,13-ratio	0.046	0.695
	9,10-ratio	0.093	0.428
Caudal-middle-frontal	12,13-ratio	0.058	0.618
	9,10-ratio	0.083	0.482
Medial-orbito-frontal	12,13-ratio	0.14	0.231
	9,10-ratio	0.127	0.276
Rostral-middle-frontal	12,13-ratio	0.03	0.797
	9,10-ratio	0.046	0.694
Superior frontal	12,13-ratio	0.022	0.849
	9,10-ratio	0.054	0.645
Superior parietal	12,13-ratio	0.057	0.625
	9,10-ratio	0.034	0.77
inferior parietal	12,13-ratio	0.121	0.302
	9,10-ratio	0.145	0.214
Lateral occipital	12,13-ratio	0.184	0.113
	9,10-ratio	0.198	0.089
Thalamus Proper	12,13-ratio	0.174	0.135
	9,10-ratio	0.216	0.063
Amygdala	12,13-ratio	0.154	0.188
	9,10-ratio	0.198	0.088
Caudal-anterior-cingulate	12,13-ratio	0.063	0.591
	9,10-ratio	0.053	0.654
Cuneus	12,13-ratio	0.088	0.451
	9,10-ratio	0.022	0.849
Frontal pole	12,13-ratio	0.019	0.868
	9,10-ratio	0.076	0.518
Insula	12,13-ratio	0.073	0.535
	9,10-ratio	0.131	0.264

Table S2. Associations between regional free water and the LA ratios in the LVS and SVS subgroups

Regional Free Water Fraction	Ratios	LVS		SVS	
		r (pearson coefficient)	p value	r (pearson coefficient)	p value
Entorhinal	12,13-ratio	0.242	0.206	0.187	0.212
	9,10-ratio	0.289	0.129	0.184	0.221
Fusiform	12,13-ratio	-0.005	0.980	0.263	0.077
	9,10-ratio	0.053	0.786	0.381*	0.009
Inferior temporal	12,13-ratio	0.086	0.658	0.301*	0.042
	9,10-ratio	0.093	0.632	0.375*	0.010
Middle temporal	12,13-ratio	-0.060	0.758	0.285	0.054
	9,10-ratio	0.058	0.764	0.438*	0.002
Superior temporal	12,13-ratio	-0.198	0.302	0.215	0.150
	9,10-ratio	-0.139	0.472	0.248	0.097
Hippocampus	12,13-ratio	-0.213	0.268	0.055	0.718
	9,10-ratio	-0.154	0.424	0.146	0.332
Caudal-middle-frontal	12,13-ratio	-0.256	0.181	0.355*	0.016
	9,10-ratio	-0.060	0.756	0.201	0.180
Rostral-middle-frontal	12,13-ratio	-0.246	0.198	0.316*	0.033
	9,10-ratio	-0.156	0.419	0.224	0.134
Medial-orbito-frontal	12,13-ratio	-0.059	0.763	0.248	0.096
	9,10-ratio	-0.012	0.949	0.189	0.209
Lateral-orbito-fronta	12,13-ratio	-0.260	0.174	0.291*	0.050
	9,10-ratio	-0.094	0.627	0.288	0.052
Superior frontal	12,13-ratio	-0.292	0.124	0.288	0.052
	9,10-ratio	-0.150	0.438	0.199	0.184
Superior parietal	12,13-ratio	-0.155	0.421	0.293*	0.048
	9,10-ratio	-0.141	0.465	0.196	0.191
Inferior parietal	12,13-ratio	-0.001	0.996	0.245	0.101
	9,10-ratio	-0.018	0.924	0.281	0.058
Lateral occipital	12,13-ratio	0.042	0.831	0.292*	0.049
	9,10-ratio	0.091	0.637	0.263	0.078
Thalamus Proper	12,13-ratio	0.145	0.454	0.114	0.451
	9,10-ratio	0.097	0.617	0.239	0.110
Amygdala	12,13-ratio	0.083	0.669	0.140	0.355
	9,10-ratio	0.066	0.733	0.232	0.121
Caudal anterior cingulate	12,13-ratio	-0.295	0.120	0.324*	0.028
	9,10-ratio	-0.107	0.580	0.134	0.376
Cuneus	12,13-ratio	0.024	0.902	0.188	0.212
	9,10-ratio	-0.051	0.794	0.100	0.509
Frontal pole	12,13-ratio	-0.079	0.682	0.107	0.480

	9,10-ratio	-0.016	0.933	0.146	0.333
Insula	12,13-ratio	-0.232	0.226	0.266	0.073
	9,10-ratio	-0.097	0.616	0.257	0.084

Table S3. Associations between regional atrophy and the ratios in the LVS and SVS subgroups

Regions	Ratios	LVS		SVS	
		r (pearson coefficient)	p value	r (pearson coefficient)	p value
Whole brain BPF	12,13-ratio	-0.056	0.767	-0.196	0.172
	9,10-ratio	-0.074	0.696	-0.157	0.276
Frontal BPF	12,13-ratio	0.017	0.930	-0.124	0.390
	9,10-ratio	0.031	0.871	-0.021	0.882
Parietal BPF	12,13-ratio	-0.203	0.281	-0.185	0.197
	9,10-ratio	-0.184	0.330	-0.138	0.338
Temporal BPF	12,13-ratio	0.051	0.788	-0.255	0.074
	9,10-ratio	-0.028	0.882	-.309*	0.029

Figure S1. Associations between 12,13-ratio and volumes of deep white matter hyperintensity (A) or periventricular volume (C). Associations between 9,10-ratio and volumes of deep white matter hyperintensity (B) or periventricular volume (D).